2017

The Mechanism of CIRP in Inhibition of Keratinocytes Growth Arrest and Apoptosis Following Low Dose UVB Radiation

Yi Liao
Chongqing University

Jianguo Feng
Chongqing University

Yi Zhang
Chongqing University

Liling Tang
Chongqing University

Shiyong Wu
Edison Biotechnology Institute

The Mechanism of CIRP in Inhibition of Keratinocytes Growth Arrest and Apoptosis Following Low Dose UVB Radiation

Yi Liao,[1,2,3] **Jianguo Feng,**[1,4] **Yi Zhang,**[1] **Liling Tang,**[1]* **and Shiyong Wu**[2]*

[1]*Key Laboratory of Biorheological Science and Technology, Ministry of Education, College of Bioengineering, Chongqing University, Chongqing, China*
[2]*Department of Chemistry and Biochemistry, 101 Konneker Laboratories, Edison Biotechnology Institute, Athens, Ohio*
[3]*Department of Cardiothoracic Surgery, Southwest Hospital, Third Military Medical University, Chongqing, China*
[4]*Department of Anesthesiology, The Affiliated Hospital of Southwest Medical University, Luzhou, Sichuan Province, China*

UV induces CIRP expression and subsequent Stat3 activation, but the biological function and mechanism of CIRP and Stat3 in mediating UVB-induced skin carcinogenesis have not been fully elucidated. In this study, we demonstrate that CIRP is elevated in all tested melanoma and non-melanoma skin cancer cell lines; and the expression of CIRP is upregulated in keratinocytes after being irradiated with relatively low dose (<5 mJ/cm^2), but not high dose (50 mJ/cm^2), UVB acutely and chronically. The increased expression of CIRP, either induced by UVB or through overexpression, leads to resistance of keratinocytes to UVB-induced growth arrest and death; and reduced expression of CIRP by RNA knockdown sensitizes keratinocyte cells to the low dose UVB radiation. We also demonstrated that CIRP expression is required for the low dose UVB-induced Tyr705-phosphorylation, but not total amount, of Stat3. The p-Stat3 level is correlated with the expression levels of cyclin D1 and VEGF, two known downstream cell growth regulators of Stat3, as well as Bag-1/S, an apoptosis regulator. Inhibition of Stat3 DNA-binding activity by S3I-201 leads to a reduction of the p-Stat3 and Bag-1/S along with growth and survival of keratinocytes post-UVB; and the effect of S3I-201 on the UVB-irradiated cells can be partially inhibited by overexpression of CIRP or Bag-1/S. Furthermore, the overexpression of Bag-1/S can totally inhibit UVB-induced PARP cleavage and caspase 3 activation. The results presented above led us to propose that CIRP-p(705)Stat3 cascade promotes cell proliferation and survival post-UVB via upregulating the expression of cyclin D1 and Bag-1/S, respectively. Published 2017. <mark>This article is a U.S. Government work and is in the public domain in the USA.</mark>

Key words: CIRP; UVB irradiation; Stat3; Bag-1/S; cell survival

INTRODUCTION

Cold inducible RNA-binding protein (CIRP) was first discovered as responding to ultraviolet light (UV)-induced DNA damage in hamster cells [1]. CIRP belongs to a family of cold shock proteins (CSPs) that responds to cold stress and functions as an RNA chaperone, which relocates from the nucleus to the cytoplasm to facilitate translation in normal cellular responses to stresses [2–4]. CIRP has been shown to protect cells from TNFα and genotoxic stress-induced cell growth arrest and apoptosis [5,6]. CIRP was also reported to be associated with inflammation and multiple kinds of tumorigenesis [7,8]. However, the regulatory function(s) of CIRP in UVB-irradiated keratinocytes is not well known. Recently, a report demonstrated that CIRP expression in liver was positively correlated with the activation of signal transducer and activator of transcription 3 (Stat3) [8], which mediates various cellular processes including cell cycle, apoptosis, and tumor angiogenesis [9,10]. The activation of Stat3 has been suggested to play critical roles in the development of skin cancer after UV exposure [11,12]. UVB induces Tyr705-phosphorylation, and thus, activation of Stat3 [13];

and constitutive activation of Stat3 is associated with a number of human tumors and cancer cell lines [14–16]. In this study, we determined the functional impact of UVB-induced CIRP expression on cell growth and survival of keratinocytes, and elucidated a novel mechanism of CIRP-regulated apoptosis.

EXPERIMENTAL PROCEDURES

Plasmids

Human CIRP cDNA was firstly cloned into the multiple cloning sites of pBluescript SK (+) between *Hind III* and *Sal I* restriction sites to construct plasmid pBS-CIRP. Plasmid pLenti-CMV-CIRP was generated by cloning the CIRP cDNA digested from plasmid pBS-CIRP into pLenti-CMV-GFP-Puro (plasmid #17448, Addgene) between *BamH I* and *Sal I* restriction sites. Plasmid pLenti-CMV-Bag-1/S was generated by inserting human Bag-1/S cDNA with *BamH I* and *XhoI* restriction digestion ends into pLenti-CMV-GFP-Puro between *BamH I* and *Sal I* restriction sites. Human CIRP and Bag-1/S cDNA was amplified by PCR using cDNA prepared from HaCaT cells. The oligonucleotide primers used in the PCR reaction for cloning of the indicated genes are listed in Table 1.

In order to stably silence CIRP expression, shRNA targeting CIRP mRNA at two different positions were devised and cloned into plasmid pLKO.1-TRC cloning vector (Addgene) between *Age I* and *EcoRI* restriction sites to form plasmid pLKO.1-CIRP-shRNA #1 and #2, respectively. A scrambled shRNA has also been designed as control (plasmid pLKO.1-scrambled-shRNA). The oligonucleotide primers sets used to generate CIRP shRNAs and scrambled shRNA control were listed in Table 2.

Cell Culture

Human keratinocyte HaCaT (a kind gift from Dr. Nihal Ahmad, University of Wisconsin–Madison), HEK-293T, A431, A375, and M624 cells were grown in Dulbecco's minimal essential medium (Cellgro, Herndon, VA) containing 10% fetal bovine serum (Atlanta Biologicals, Flowery Branch, GA), 100 U/ml penicillin, and 100 µg/ml streptomycin (Cellgro) at 37°C with 5% CO_2. For cells stably expressing CIRP, Bag-1/S, CIRP shRNA, or scrambled shRNA, the medium was supplemented with 1.0 µg/ml puromycin (Sigma–Aldrich, St. Louis, MO).

UVB Irradiation and Drug Treatments

UVB was generated as described in our previous report [17]. The dose rate for 3, 5, 7, or 10 mJ/cm^2 of UVB radiation was 0.6, 1.0, 1.4, or 2.0 mW/s,

respectively. Medium was removed before UVB irradiation. Immediately after UVB exposure, fresh medium was added to cells for culture until harvest. S3I-201 (Sigma–Aldrich) was directly added to fresh medium in the designated concentrations and was continuously incubated with cells until harvest. For combinatorial treatment, S3I-201 was directly added into fresh medium to a final concentration of 100 µg/ml immediately after UVB exposure and was continuously incubated with cells until harvest.

RNA Interference (RNAi)

HaCaT cells were grown overnight to approximately 40% confluence and transiently transfected with human CIRP short interfering RNA (siRNA): GUACGGACAGAUCUCUGAAdTdT (Sigma–Aldrich) [18], Bag-1 siRNA (sc-29211, Santa Cruz Biotechnology, Inc.), or non-targeting siRNA (FITC Conjugate)-A (sc-36869, Santa Cruz Biotechnology Inc., Santa Cruz, CA). Transfection was performed with Lipofectamine RNAi MAX reagent (Invitrogen, Carlsbad, CA) according to the manufacturer's instructions.

Establishment of Stable Cell Lines

CIRP-deficient stable cell lines and the control cell line were established by lentiviral transduction with CIRP-shRNA constructs specific for human CIRP or scrambled shRNA constructs (pLKO.1-CIRP-shRNA #s or pLKO.1-scrambled-shRNA). In brief, HEK-293T packaging cells were co-transfected with lentiviral shRNA constructs as well as lentiviral helper vectors pCMV-VSV-G plasmid (Addgene, Cambridge, MA) and pCMV-dR8.2 dvpr plasmid (Addgene). After 48 h incubation, the viral supernatant fraction was collected. HaCaT cells were infected with lentiviral particles for 24 h and then selected with puromycin over 1 wk. Plasmids were transected using Effectene Transfection Reagent (QIAGEN, Germantown, MD) according to the manufacturer's protocol.

HaCaT cell lines overexpressing GFP, CIRP, or Bag-1/S (referred to as Le/GFP, Le/CIRP, or Le/Bag-1/S) were established by lentiviral transduction with each cDNA construct (pLenti-CMV-GFP, pLenti-CMV-CIRP, or pLenti-CMV-Bag-1/S) using the same method as described above.

Table 1. Oligonucleotide Primers Used in PCR Reaction for Cloning Indicated Genes Into Overexpression Plasmids

Gene	Direction	Primer sequence (5' to 3')
CIRP[a]	Forward	CCC<u>AAGCTT</u>ATGGCATCAGATGAAGGCAAAC
	Reverse	ACGC<u>GTCGAC</u>GTCAGGCTGGGTTTGACAAGA
Bag-1/S[b]	Forward	CGC<u>GGATCC</u>GCGAAGAGATGAATCGGAGC
	Reverse	CCG<u>CTCGAG</u>CTGCTACACCTCACTCGGCCA

All restriction sites are underlined.
[a]Includes a *Hind III* or *Sal I* restriction site for ligation into pLenti CMV GFP Puro plasmid.
[b]Includes a *BamH I* or *XhoI* restriction site for ligation into pLenti CMV GFP Puro plasmid.

Table 2. Oligonucleotide Primer Sets Used to Generate Scrambled shRNA Control and CIRP shRNAs

shRNA	Direction	shRNA Sequence (SCR and target sequence underlined)
SCR shRNA	Forward	5′-CCGGG<u>GCGATGTGGCGAACTGACACG</u>CTCGAG<u>CGTGTCAGTTCGCCACATCGC</u>TTTTTG-3′
	Reverse	5′-AATTCAAAAA<u>GCGATGTGGCGAACTGACACG</u>CTCGAG<u>CGTGTCAGTTCGCCACATCGC</u>-3′
CIRP shRNA #1	Forward	5′-CCGG<u>AGTACGGACAGATCTCTGAAG</u>CTCGAG<u>CTTCAGAGATCGTCCGTACT</u>TTTTTG-3′
	Reverse	5′-AATTCAAAAA<u>AGTACGGACAGATCTCTGAAG</u>CTCGAG<u>CTTCAGAGATCGTCCGTACT</u>-3′
CIRP shRNA #2	Forward	5′-CCGGG<u>GGAGTCAGAGTGGTGGCTACA</u>CTCGAG <u>TGTAGCCACCACTCTGACTCC</u>TTTTTG-3′
	Reverse	5′-AATTCAAAAA<u>GGAGTCAGAGTGGTGGCTACA</u>CTCGAG <u>TGTAGCCACCACTCTGACTCC</u>-3′

Western Blot Analysis

Cells were lysed using cold NP-40 buffer (100 mM Tris, pH 7.4, 80 mM NaCl, 10 mM EDTA, 0.5% Nonidet P-40, 0.1% SDS) with proteinase inhibitor mixture (Sigma–Aldrich). Cell lysate was incubated on ice for 30 min with shaking every 5 min and then centrifuged at 16 000 rpm at 4°C for 10 min. Protein concentration was measured by DC protein assay kit (Bio-Rad Laboratories). Equal amounts of protein were resolved on SDS–PAGE and transferred to nitrocellulose membrane (Invitrogen). The membrane was then blocked with 5% milk in Tris-buffered saline plus Tween 20 (TBST) for 1 h and then incubated overnight at 4°C with primary antibody, followed by incubation with a corresponding horse-radish peroxidase-conjugated secondary antibody (Santa Cruz Biotechnology, Inc.). Membrane was developed in West Pico Super Signal chemiluminescent substrate (Pierce). Primary antibodies used were as follows: anti-CIRP, anti-beta actin, anti-cyclin D1, anti-c-Myc, anti-VEGF (Source: rabbit. Santa Cruz Biotechnology, Inc.) anti-PARP, anti-cleaved caspase-3, anti-Bag-1, anti-Stat3, anti-p-Stat3 (Source: mouse. Cell Signaling Technology, Danvers, MA). For relative quantification, the integrated optical density (IOD) was estimated using ImageJ (NIH). Relative protein expression level was calculated as IOD Experimental/ IOD Control.

Total RNA Isolation, cDNA Synthesis, and PCR

Total RNA was harvested using QIAshredder and RNeasy Kit (both from QIAGEN) according to the manufacturer's protocol. A total of 1.0 μg RNA was reverse-transcribed with the SuperScript™ III Reverse Transcriptase kit (Invitrogen) using the manufacturer's protocol. PCR was performed on the first strand of cDNA with the primers listed in Table 1 by using the Phusion reaction system (Thermo Scientific, Waltham, MA).

Immunofluorescence Staining

Cells were fixed with 4% paraformaldehyde for 15 min at room temperature, washed with PBS three times, and permeabilized with 0.2% Triton X-100 in PBS for 5 min. Cells were then blocked with blocking solution (2 mg/ml BSA in PBS) for 45 min before incubating with rabbit anti-CIRP polyclonal antibody (sc-133460, Santa Cruz Biotechnology, Inc.) for 1 h. After washing five times with PBS, cells were incubated with a Cy3-conjugated IgG Fraction monoclonal mouse anti-rabbit IgG (Jackson ImmunoResearch, West Grove, PA) for 1 h at RT. After being washed five times with PBS, a drop of Antifade mount fluid with DAPI (Invitrogen) was added to cells. Pictures were taken using a NIKON Eclipse E600.

Clonogenic Assay

Cells were seeded at a density of 1000 cells/well in a 6-well plate and incubated overnight. Then cells were subjected to designated amounts of UVB irradiation. Immediately after treatment, fresh medium was added to cells and they were incubated for another 2 wk without disturbance. After washing two times with PBS, cells were fixed with cold methanol for 15 min at RT and then stained by 0.4% crystal violet in 25% methanol for another 30 min following by three washes with distilled water. Photos were taken by Kodak IS in vivo F system and only colonies with size greater than 0.4 mm were counted.

Cell Proliferation Assay

HaCaT cell proliferation was assessed using a MTT based in vitro toxicology assay kit (Sigma–Aldrich). Briefly, HaCaT cells were plated at a density of 1×10^5 cells/well in 6-well plate and incubated overnight. The cells were then sham or UVB irradiated. At designed time-points, MTT solution (1:10 dilution) was added to and incubated with the cells for 3 h before measuring absorbance at 570 nm.

Cell Cycle Analysis

A sum of 10^5 HaCaT (Le/GFP, Le/CIRP, Le/scrambled shRNA, Le/CIRP shRNA #1, and Le/CIRP shRNA #2) cells were seeded in each well of a 6-well plate and cultured for 24 h. The cells were then harvested and fixed with cold 75% ethanol at 4°C overnight. After incubation with RNaseA (100 mg/L, Sigma–Aldrich) for 10 min, the cells were stained with propidium iodide (PI, 50 mg/mL, Sigma–Aldrich) for cell cycle analysis by flow cytometry (FACSAria™ II, BD Biosciences, Sparks, MD). Cell cycle distributions were determined with Motif Software.

Cytotoxicity Assay of S3I-201

Cytotoxicity of the Stat3-specific inhibitor, S3I-201, on HaCaT cells was analyzed using the Pierce LDH Cytotoxicity Assay Kit (Thermo Scientific). Briefly, HaCaT cells were placed in a 96-well plate at a density of 5×10^3 cells/well. Then the cells were treated with 0–300 μM of S3I-201 for 24 h. The LDH (lactate dehydrogenase) activity in the medium was determined by measuring absorbance at 450–690 nm. The maximum LDH activity served as control was determined by adding 10 μl lysis buffer to the well before measuring the absorbance.

Xenografts Generation

All procedures for animal experiments were approved by the Committee on the Use and Care on Animals (The Third Military Medical University, Chongqing, China) and performed in accordance with the institution guidelines. HaCaTt and HaCaT tumor xenografts were established by subcutaneously inoculating 1×10^6 cells into the both flanks of 6-wk-old BALB/c nude mice (HaCaTt group, $n = 7$; HaCaT group, $n = 7$). Twenty-eight days later, animals were sacrificed to weight the established tumors. All animals received humane care according to the criteria outlined in the "Guide for the Care and Use of Laboratory Animals" prepared by the National Academy.

Immunohistochemistry

Streptavidinbiotin peroxidase complex method was used for immunohistochemical staining on formalin-fixed, paraffin-embedded tissue sections. Rabbit anti-human CIRP antibody (1:250) were added for 1 h at 37 and 4°C overnight. Signals were visualized using the 3,3′-diaminobenzidine substrate solution (DAKO) and light counterstaining with hematoxylin.

Statistics

The data were expressed as the mean ± SD. The statistical significance of differences for the mean values of groups was determined with Student's *t*-test. Differences with a *P*-value of less than 0.05 were considered significant.

RESULTS

CIRP Expression Is Induced in Skin Cancer Cells and in Keratinocytes Exposed to Lower-Dose But Not Higher-Dose UVB Radiation

To determine the potential correlation of CIRP expression and UVB-induced skin cancer formation, we first analyzed the expression levels of CIRP in keratinocyte and skin cancer cells. Our data indicated that compared to keratinocyte HaCaT cells, CIRP expression in squamous carcinoma A431 cells as well as melanoma M624 and A375 cells was increased by

approximately 120%, 44%, and 126%, respectively (Figure 1A). The expression of CIRP in HaCaT cells was reduced by 19% but increased by 80% after exposing the cells to 50 or 3 mJ/cm² of UVB, respectively (Figure 1B); while the expression of CIRP is not effected in the cancer cells by the same dose of UVB (3 and 5 mJ/cm²) (data not shown). The induced expression of CIRP was accompanied with a cytosolic translocation of the protein, which has been shown to be important for some CIRP-facilitated mRNA translation in stress response, in HaCaT cells after the UVB (3 mJ/cm²) exposure (Figure 1C). These results demonstrate for the first time that CIRP was upregulated in various human skin cancer cells and might play a role in regulation of oncogenic signaling in keratinocytes receiving low-dose UVB irradiation.

CIRP Expression Is Increased in Transformed Keratinocytes

To further investigate the correlation between CIRP expression and UVB-induced skin cancer formation, we generated an UVB-transformed keratinocyte cell line (HaCaTt) by irradiating HaCaT cells with UVB (3 mJ/cm²) once every other day for 3 wk. After recovering for 1 wk after UVB treatment, the expressions of CIRP and other oncogenic protein markers in HaCaTt cells were analyzed using western blot analysis. Our data indicated that CIRP expression was increased in HaCaTt cells in comparison with its expressions in HaCaT cells (Figure 2A). The increased expression of CIRP was correlated with increased expressions of c-Myc, VEGF, and cyclin D1 as well as phosphorylation (Tyr705) of Stat3 (Figure 2A). Our data further indicated that the HaCaTt cells with higher CIRP expression were more resistant to UVB (3–10 mJ/cm²) induced cell growth arrest (Figure 2B) and to single dose UVB-induced cell death (Figure 2C). The increased transformation potential of HaCaTt cells were confirmed using animal model. Our data showed that while HaCaT cells only formed small tumors in only 28.6% of the mice, HaCaTt cells formed relatively large tumors in 100% of the mice (Figure 3A). The average weight of tumors was significantly lower in HaCaT groups than that in HaCaTt group (Figure 3B). Immunohistochemical staining analysis revealed extensive expression of CIRP in tumors from HaCaTt group (Figure 3C). These results suggest that CIRP might contribute to chronic low-dose UVB exposure induced oncogenic transformation of keratinocytes through its role in regulation of cell proliferation and survival.

CIRP Deficiency Sensitizes Keratinocytes to UVB Radiation

To further investigate the role of CIRP in regulation of cell proliferation and survival after UVB radiation, we generated two CIRP deficient HaCaT cell lines with a partial knockdown (shRNA #1) or a potent loss (shRNA #2) of CIRP expression (Figure 4A). Our data indicated that while c-Myc and Bcl-2 levels were not
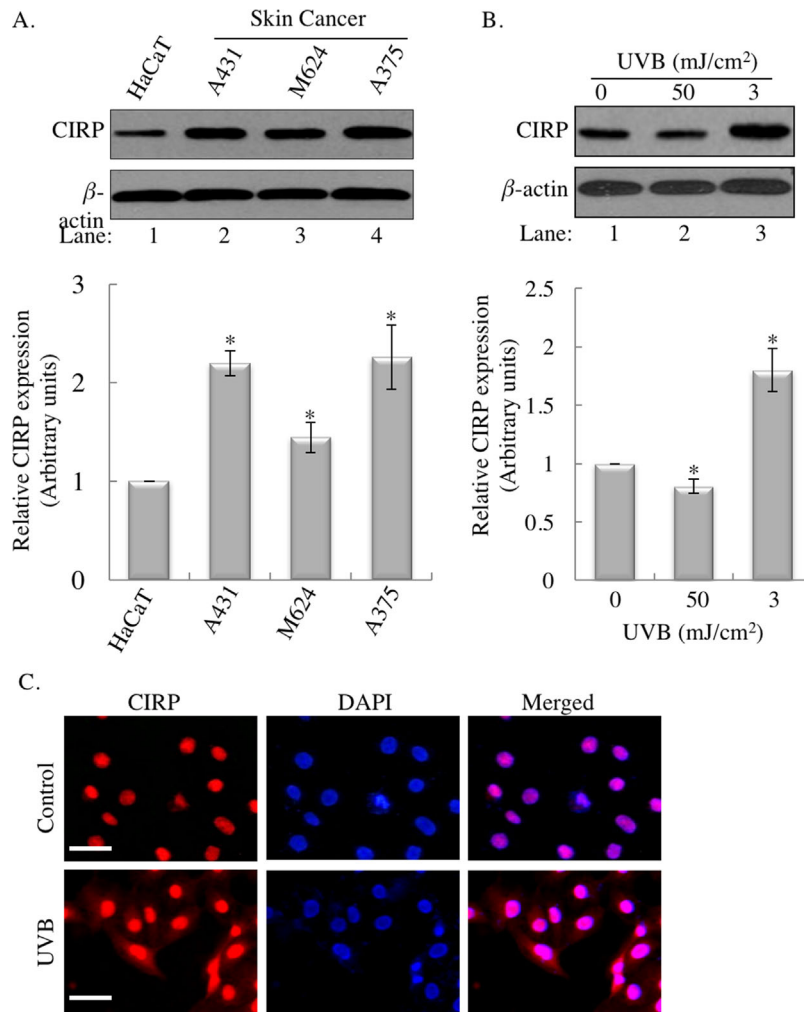
Figure 1. CIRP expression is increased in skin cancer cells and UVB irradiated keratinocyte cells. (A and B) Western blot analyses of CIRP expression in HaCaT and skin cancer cell lines; and in HaCaT cells at 6 h post-UVB. (B) and densities in the western blot was quantitative analyzed using ImageJ (NIH). *P < 0.01 versus HaCaT cells without UVB treatment. (C) Localization of CIRP(red) in HaCaT cells at 24 h after sham or UVB treatment. Nuclei were stained by DAPI (blue). Scale bars: 50 μm. All figures represent the average of three sets of independent experiments.

significantly changed, cyclin D1 level was correlatively reduced as CIRP level reduced (Figure 4A, Lanes 3 vs. 2 vs. 1) suggesting cyclin D1 might be involved in CIRP-mediated regulation of cell proliferation. Cell cycle analysis revealed that silencing CIRP expression in HaCaT cells caused moderate G2/M arrest (Figures 4B and Supplementary S1). Furthermore, because our data indicated that while the CIRP knockdown inhibited HaCaT cell growth (Figure 4C, top left panel), it also sensitized the cells to lower dose (3 and 5 mJ/cm^2) UVB irradiation (Figure 4C, top right and bottom left panels), but not to relatively higher dose (10 mJ/cm^2) (Figure 4C, bottom right panels), we determined whether the reduced cell numbers after UVB irradiation were partially contributed by sensitizing the cells to UVB-induced death. Our data showed that Stat3 phosphorylation was correlated

with CIRP expression (Figure 2A) but Bcl-2 was not changed in CIRP knockdown cells (Figure 4A), so we analyzed the expression of Bag-1, a regulator of Bcl-2 [19], in CIRP transient knockdown HaCaT cells in the absence or presence of UVB. Bag-1 has three isoforms including the largest isoform p50: Bag-1/L; the intermediate isoform p46: Bag-1/M; and the most abundant isoform p36: Bag-1/S [20]. Our data indicated that along with the reduced Tyr705-phosphorylation of Stat3, the expressions of all three isoforms of Bag-1 were suppressed in CIRP siRNA knockout HaCaT cells (Figure 5A, Lanes 5 vs. 1). In addition, our data showed that the expression of Bag-1/S, but not Bag-1/L and M, in correlation with the phosphorylation of Stat3, was reduced in both cell lines at 6 h and then increased at 24 h post-UVB (Figure 5A). However, the levels of Bag-1/S expression
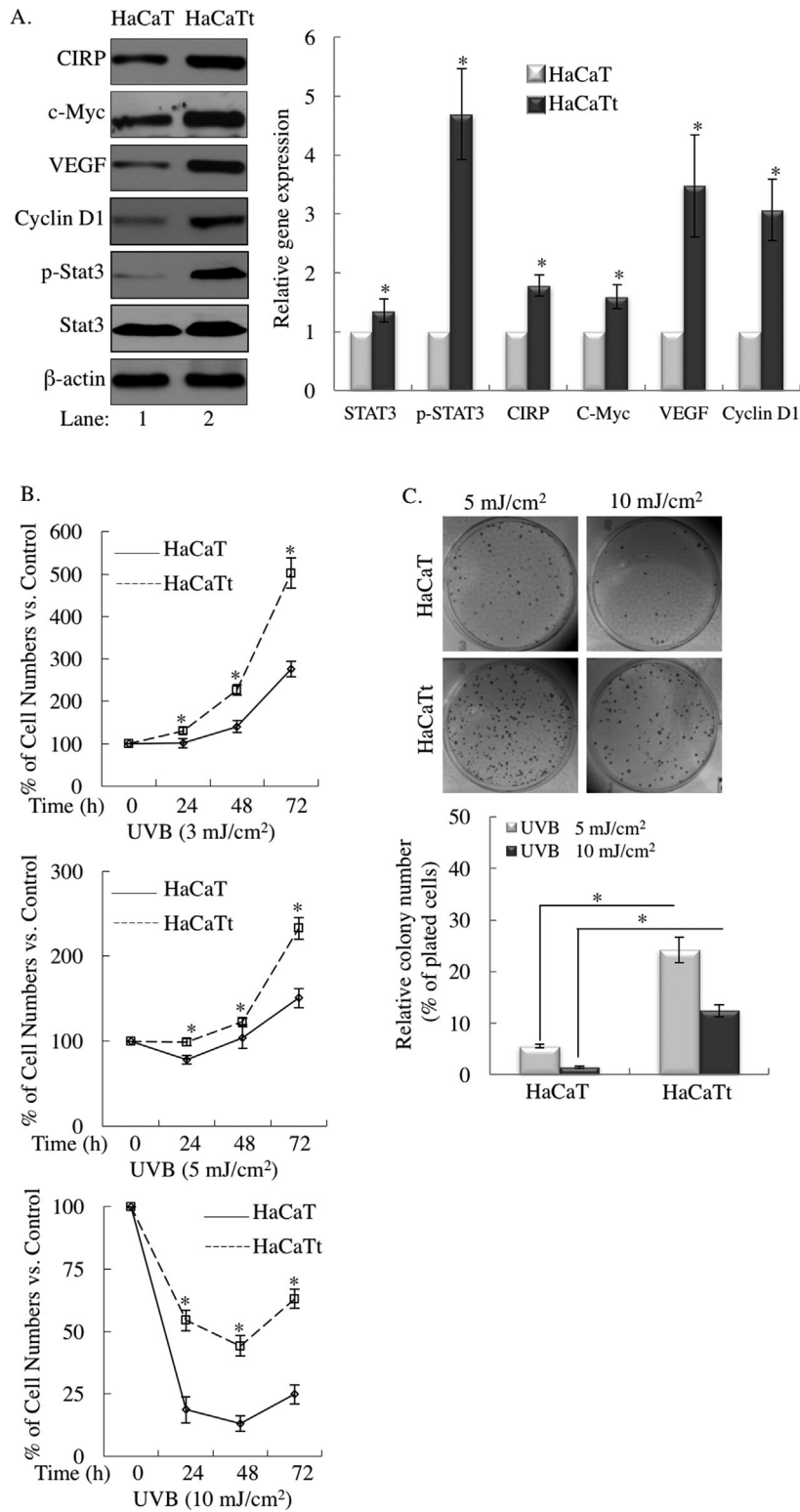
Figure 2. Chronic low-dose UVB exposure increased CIRP expression and UVB resistance of HaCaT cells. (A) Western blot analysis of the expression levels of indicated genes in HaCaT and UVB-transformed HaCaT (HaCaTt)cells. (B) and densities in the western blot was quantitative analyzed using ImageJ (NIH). *$P < 0.01$ versus HaCaT cells. (B) Cell viability determined by MTT assay. Data were expressed as mean $\pm$ SD (error bars) from there independent experiments. *$P < 0.01$ HaCaT cells. (C) Clonogenic survival assay. A sum of 1000 each of HaCaT or HaCaTt cells were seeded, UVB irradiated, and cultured for 2 wk before the colonies were counted. *$P < 0.01$ versus HaCaT cells treated with same dose of UVB. All figures represent the average of three sets of independent experiments.
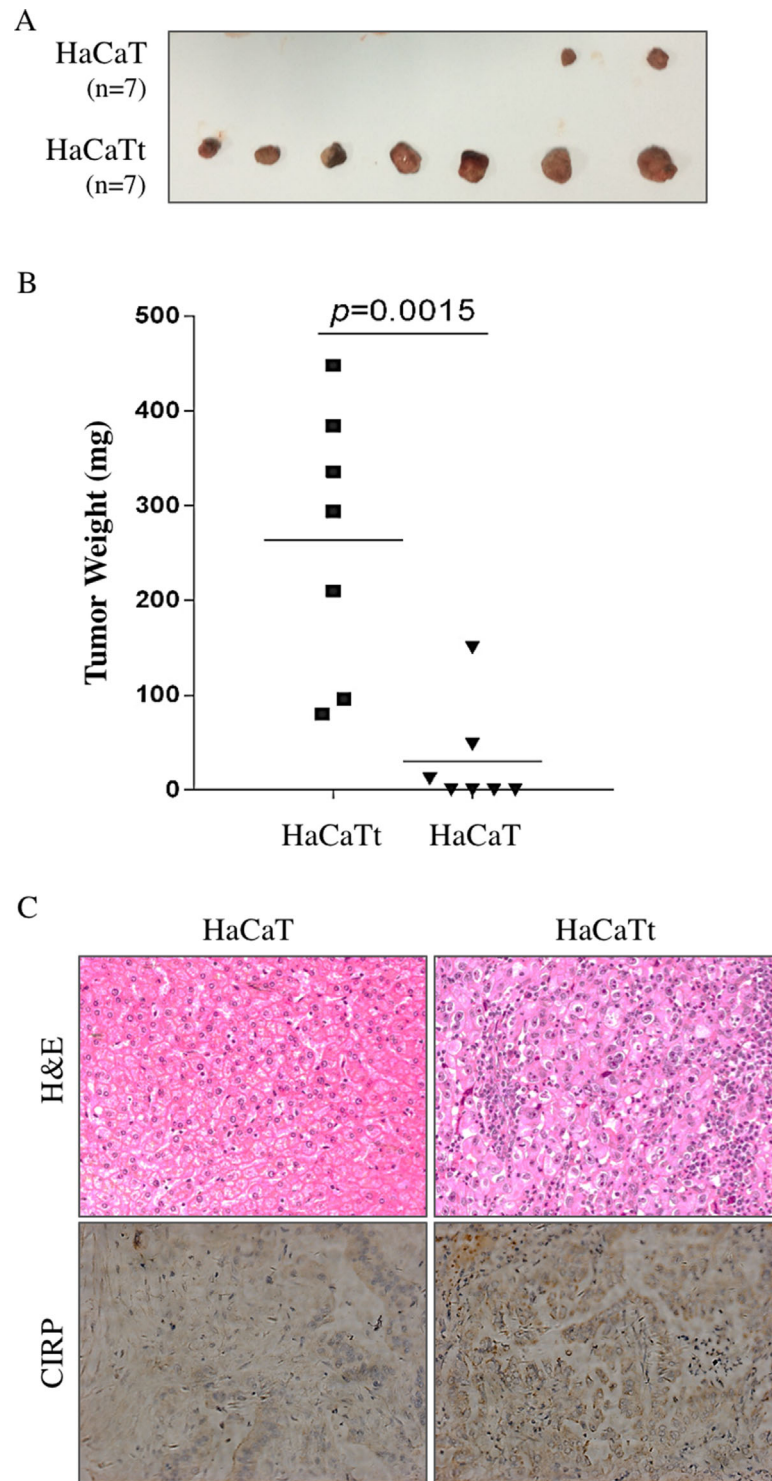
Figure 3. Chronic low dose UVB treatment promotes the in vivo Tumorigenic Capacity of HaCaT Cells. (A) HaCaT and HaCaTt cells were subcutaneously inoculated in BALB/c nude mice ($n = 7$ for both group). At 28 d after inoculation, tumors were surgically removed. (B) The weight of established tumors was measured and is shown in a scatter plot. Horizontal lines indicated the average values. (C) Representative images showing CIRP expression was analyzed by immunohistochemical on tumor xenografts (magnification × 200).
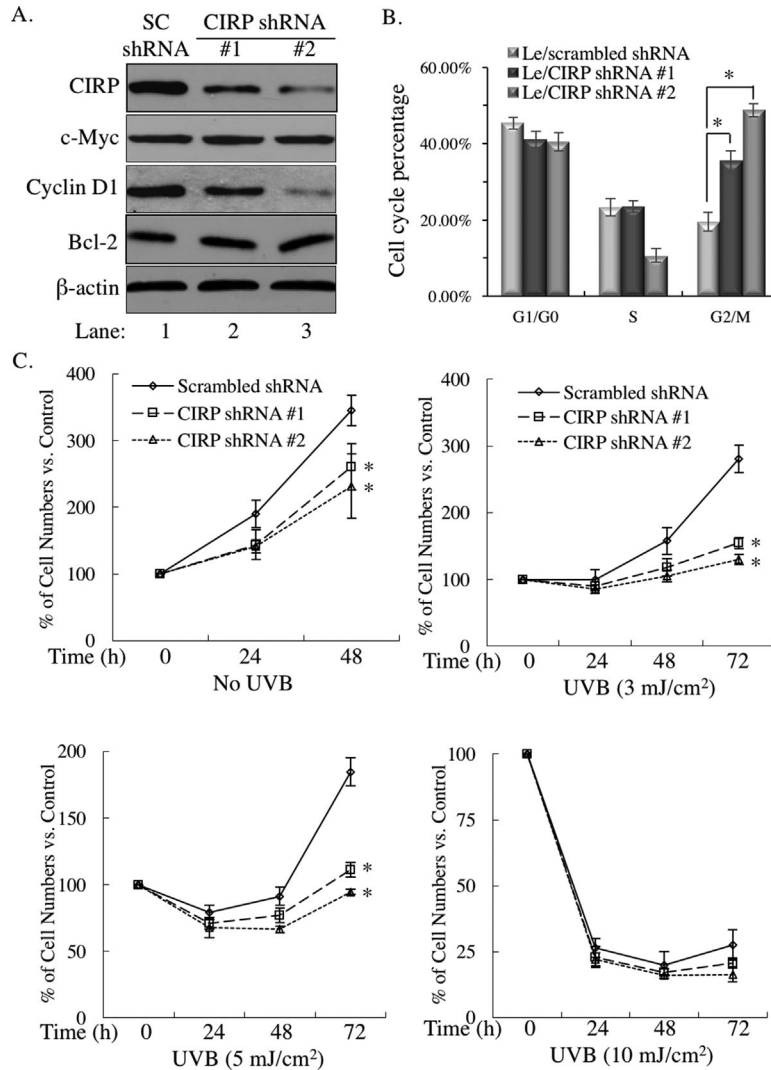
Figure 4. Effect of CIRP knockdown on HaCaT cell proliferation and survival after various doses of UVB irradiation. (A) Western blot analysis of the expression levels of indicated genes in CIRP stable knockdown cell lines. (B) Cell cycle analysis was performed on same cell lines at 24 h after seeding. The population percentages at G0/G1, S and G2/M phases are shown as mean $\pm$ SD from three independent experiments ($*P < 0.05$). (C) Control (scramble) or CIRP-deficient cells were UVB irradiated with various dosages. Cell viability at indicated time post-UVB was measured using the MTT assay. Results are mean $\pm$ SD (error bar) from three independent experiments. $*P < 0.05$ versus control.

and Tyr705-phosphorylation in the CIRP knockdown cells were much lower than the ones in the control cells (Figure 5A, Lanes 5–8 vs. 1–4). The growth of the CIRP knockdown cells was also much slower than the control cells (Figure 5B). These results suggested that CIRP might play a critical role in the regulation of cell survival in response to low dose UVB radiation via the Stat3 phosphorylation-regulated Bag-1/S signaling cascade.

CIRP Overexpression Desensitizes Keratinocytes to UVB Irradiation

To further investigate the role of CIRP in regulation of keratinocyte growth and recovery after UVB irradiation, we established GFP or CIRP stably transfected HaCaT cell lines Le/GFP and Le/CIRP. Our data showed that CIRP overexpression could lead to an increase in the Stat3 Tyr705-phosphorylation without altering the expression as well as increased Bag-1 and cyclin D1 expression (Figure 6A). Our data also demonstrated that compared to the control Le/GFP cells, Le/CIRP cells had a higher proliferation rate (Figure 6B top panel) and recovered faster (Figure 6B, bottom panel) after UVB irradiation. Overexpression of *CIRP* in HaCaT cells resulted in the accelerated G2/M transition (Figures 6C and Supplementary S1). These results indicated that CIRP expression is not only sufficient to stimulate proliferation but might also promote survival of keratinocytes in the presence and absence of UVB irradiation.

A.

*: p<0.05 vs. NS control at 0 h
#: p<0.05 vs. CIRP KO at 0 h

B.
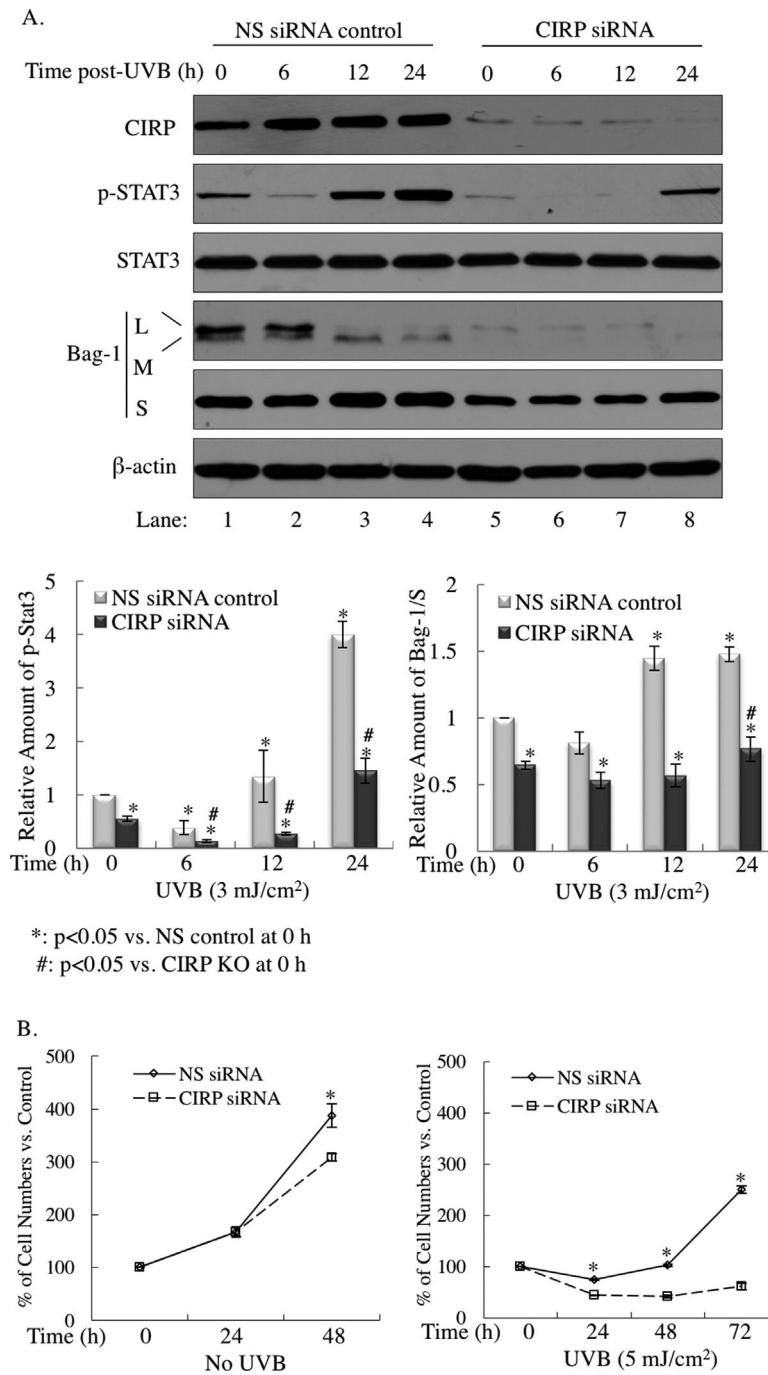
Figure 5. CIRP deficiency sensitizes HaCaT cells to low-dose UVB irradiation. (A) Western blot analysis of the expression levels of indicated genes in HaCaT cells that were transfected with NS control or CIRP siRNA post-UVB irradiation. Relative levels of phosphorylated STAT3 and Bag-1/S were quantitatively analyzed using ImageJ (NIH). Results are the mean $\pm$ SD (error bar) from three independent experiments. *$P < 0.01$ versus 0 h NS siRNA control; #$P < 0.05$ versus 0 h CIRP siRNA. (B) Control (NS siRNA) or CIRP siRNA transfected HaCaT cells were sham or UVB irradiated. Cell viability at indicated time post-UVB was measured using the MTT assay. Results are mean $\pm$ SD (error bar) from three independent experiments. *$P < 0.05$ versus NS siRNA.

UVB-Induced Bag-1/S Elevation in HaCaT Cells Requires Stat3 Activity

Because the level of Stat3 Tyr705-phosphorylation was correlated to the expression of CIRP or Bag-1/S at some points in cells with or without UVB exposure (Figure 5A), we examined whether p-Stat3 is involved in regulation of CIRP and Bag-1/S expression via upstream and/or downstream signaling pathways post-UVB. First, a specific Stat3 inhibitor S3I-201,

which inactivates Stat3 by blocking its phosphorylation and dimerization [21], was used to determine the role of Stat3 activity in regulation of CIRP and Bag-1/S expressions. Our data indicated that S3I-201 inhibited Stat3 phosphorylation in a concentration dependent manner with an IC_{50} at the concentration of $100 \mu M$ (Figure 7A). Our data also showed that S3I-201, at a concentration of $100 \mu M$, had no significant effect on the expression of Stat3 (Figure 7A, Lane 3) and did not present statistically significant cytotoxicity in HaCaT cells (Figure 7B). In correlation with the reduction of p-Stat3, the level of Bag-1/S, but not CIRP, was also gradually reduced upon increasing the

concentration of S3I-201 (Figure 7A) likely indicating that Bag-1/S is downstream and CIRP is upstream of p-Stat3.

CIRP-Stat3-Bag-1/S Cascade Regulates Growth/Survival of Keratinocytes Post-UVB

To investigate functional relationships among CIRP, p-Stat3, and Bag-1/S, we generated a stable Bag-1/S overexpressed HaCaT cell line, Le/Bag-1/S (Figure 8A), and used it along with Le/GFP and Le/CIRP cells to study their roles in regulation of cell proliferation and survival after UVB irradiation. Our data showed that the levels of p-Stat3 and Bag-1/S
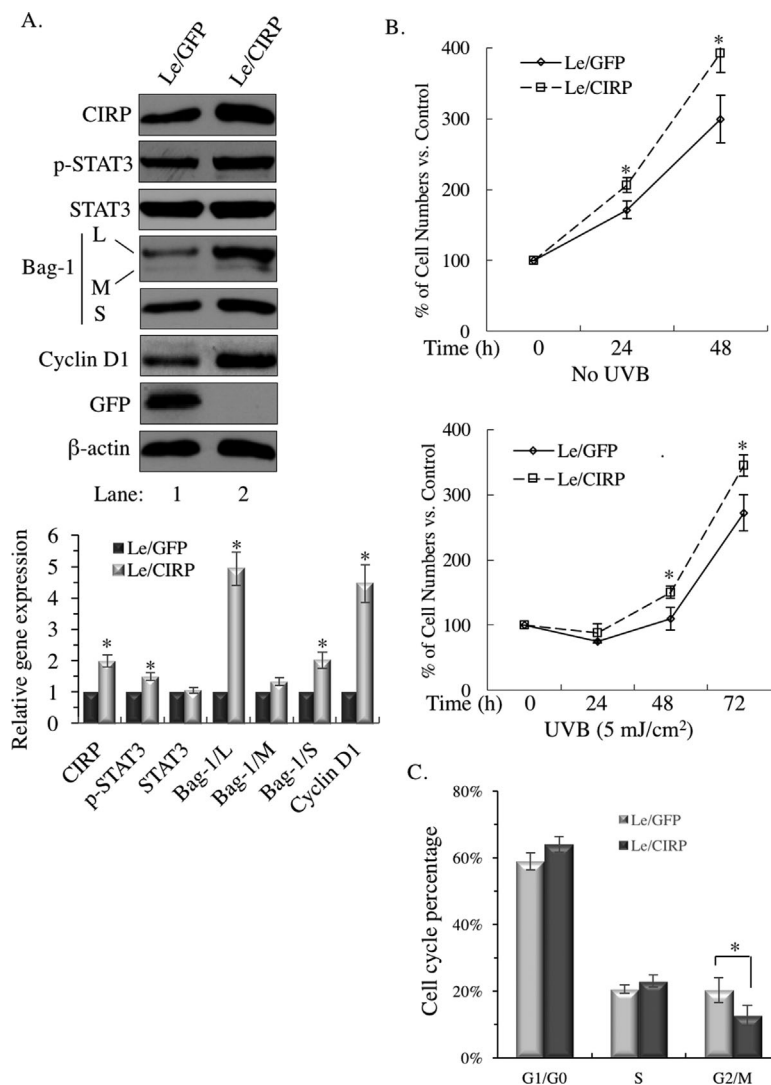
Figure 6. CIRP stable overexpression HaCaT cells are more resistant to low-dose UVB irradiation. (A) Western blot analysis of the expression levels of indicated genes in HaCaT cells that were infected with GFP (Le/GFP) or CIRP (Le/CIRP) lentiviral particles. (B) Le/GFP and Le/CIRP cells were sham or UVB irradiated. Cell viability at indicated time post-UVB was measured using the MTT assay. Results are mean ± SD (error bar) from three independent experiments. *$P < 0.05$ versus Le/GFP cells. Cell cycle analysis was performed on Le/GFP and Le/CIRP cells at 24 h after seeding. The population percentages at G0/G1, S and G2/M phases are shown as mean ± SD from three independent experiments (*$P < 0.05$).

were increased in Le/GFP and Le/CIRP cells (Figure 8B, Lanes 2 vs. 1; 6 vs. 5; Table 3), but not in Le/Bag-1/S cells (Figure 8B, Lanes 10 vs. 9; Table 3), after UVB irradiation. The Tyr705-phosphorylation of Stat3 was significantly decreased in all three cell lines after S3I-201 treatment with or without UVB treatment (Figure 8B, Lanes 3, 4, 7, 8, 11, 12; Table 3), along with a reduced expression of Bag-1/S in both Le/GFP and Le/CIRP cells (Figure 8B, Lanes 3 vs. 1; 7 vs. 5; Table 3) but not statistically significantly in Le/Bag-1/S cells (Figure 8B, Lanes 11 vs. 9; Table 3). These results indicated that the background and UVB-induced expression of Bag-1/S is dependent on the Tyr705-phosphorylation of Stat3.

To further analyze the physiological role of the CIRP/p-Stat3/Bag-1/S cascade in regulation of UVB-irradiated keratinocytes, we analyzed the populations of Le/GFP, Le/CIRP, and Le/Bag-1/S cells 24 h after being treated with UVB and/or S3I-201. Our data showed that in comparison with the untreated Le/GFP cells, all three cell lines revealed an approximate 40% reduction in cell population at 24 h after

S3I-201 (100 μM) treatment (Figure 8C, Samples 7–9 vs. 1). Compared to the control Le/GFP cells, over-expression of CIRP increased the population of Le/CIRP cells in the absence or presence of UVB irradiation (Figure 8C, Samples 2 vs. 1; 5 vs. 4). However, the increased population of Le/CIRP cells in the absence or presence of UVB irradiation was diminished or reduced when the cells were treated with S3I-201 (100 μM) (Figure 8C, Samples 8 vs. 7; 11 vs. 10) indicating the Tyr705-phosphorylation of Stat3 is a downstream factor of CIRP in regulation of cell growth post-UVB. Our data also showed that while overexpression of Bag-1/S did not have an effect on cell population in the absence or presence of S3I-201 (Figure 8C, Samples 3 vs. 1; 9 vs. 7), it increased cell population when the cells received UVB irradiation (Figure 8C, Samples 6 vs. 4; 12 vs. 10) indicating Bag-1/S could be a downstream factor in p-Stat3-mediated cell growth arrest and/or death signaling pathway upon UVB irradiation. Furthermore, our data indicated that while the population of Le/CIRP cells was higher than Le/Bag-1/S cells after UVB irradiation (Figure 8C, Samples 5 vs. 6); the population of Le/CIRP cells appears to be similar or less than Le/Bag-1/S cells after the combined treatments of S3I-201 and UVB (Figure 8C, Samples 11 vs. 12). These results further demonstrated that CIRP is upstream of Bag-1/S and suggested that other CIRP downstream factor(s), such as cyclin D1, is in coordination with Bag-1/S in regulation of cell growth and survival post-UVB.

CIRP or Bag-1/S Regulates UVB-Induced Apoptosis of Keratinocytes

To determine whether inhibition of apoptosis is one of the mechanisms that increased the population of Le/CIRP and Le/Bag-1/S cells post-UVB, we analyzed the effect of CIRP or Bag-1/S targeting siRNA knockdown on cleavages of PARP and caspase-3 in HaCaT cells after UVB irradiation. In order to trigger a distinct apoptotic process without killing all the cells, we used a UVB dose of 7 mJ/cm² for the experiment. Our data showed that while CIRP knockdown decreased the expression of Bag-1/S in the absence or presence of UVB irradiation (Figure 9A), Bag-1/S knockdown had no statistically significant effect on the expression of CIRP with or without UVB irradiation (Figure 9B) confirming our conclusion that Bag-1/S is downstream of CIRP. Furthermore, our data showed that while having no effect on PRAR cleavage and caspase 3 activation without UVB treatment (Figure 9A and B, Lane 3), either CIRP or Bag-1/S knockdown increased the ratio of cleaved PARP/PARP and cleaved caspase 3 post-UVB irradiation (Figures 9A and 8B, Lane 4). Interestingly, the CIRP or Bag-1/S knockdown had a very similar effect on PARP and caspase 3 post-UVB (Figure 9A Lane 4 vs. B 4), suggesting that Bag-1/S might be a CIRP
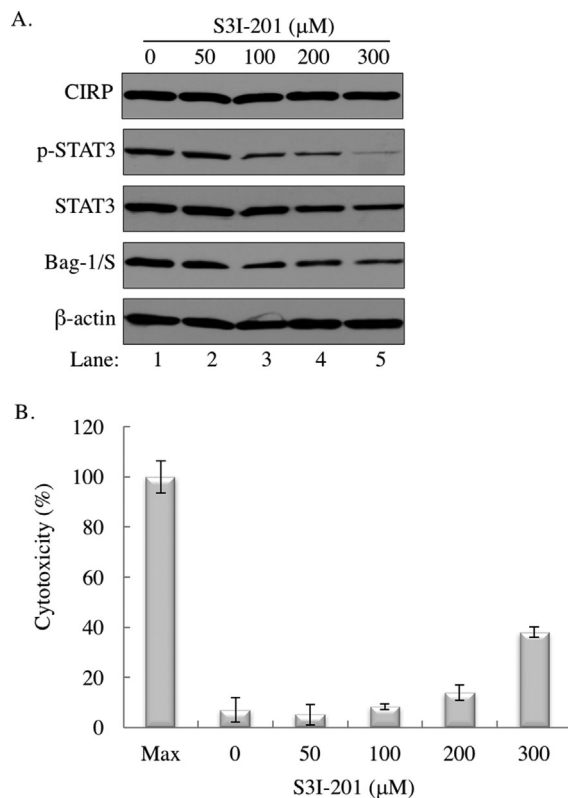
Figure 7. Effect of Stat3 inhibitor S3I-201 on CIRP and Bag-1/S expression. (A) Western blot analysis of the expression levels of indicated genes in HaCaT cells after being treated with various concentrations of S3I-201 for 24 h. (B) HaCaT cells were treated with various concentrations of S3I-201. The cytotoxicity of S3I-201 was determined at 24 h post-treatment by measuring lactate dehydrogenase activity in the medium.

A.

B.

C.
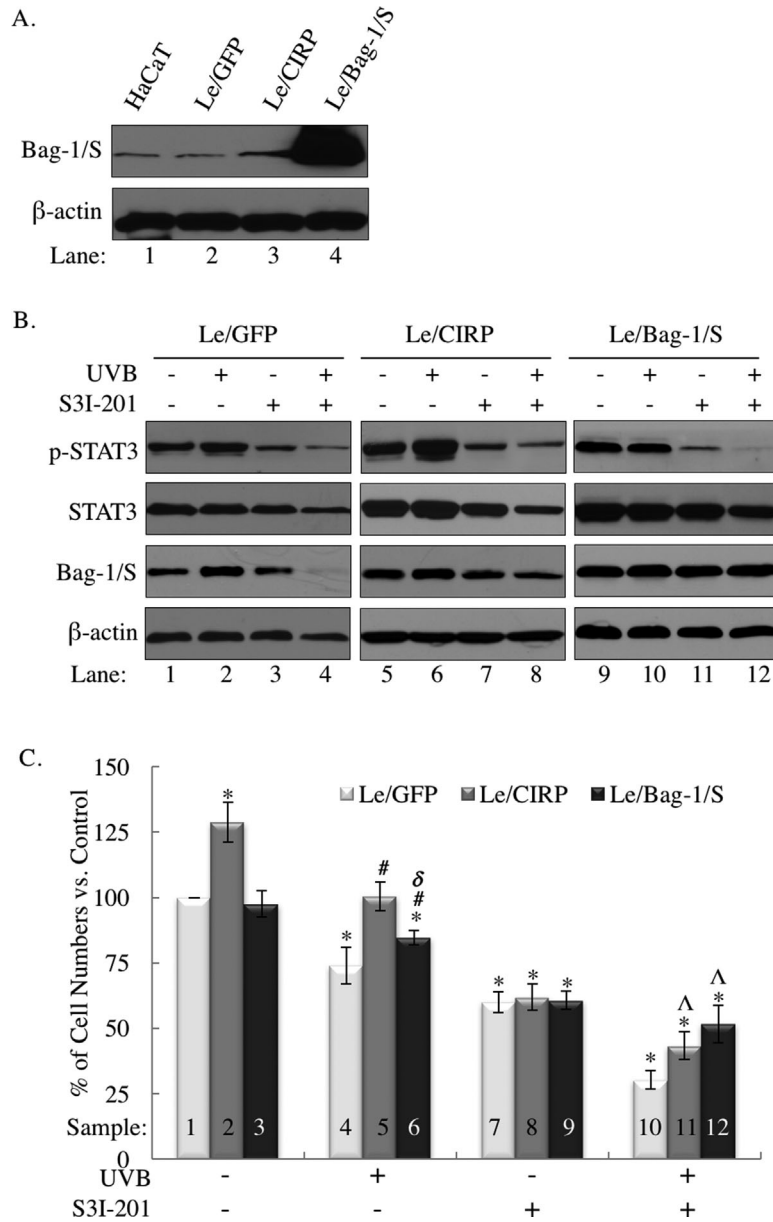
Figure 8. CIRP-Stat3-Bag-1/S cascade regulates HaCaT cell proliferation and survival after low-dose UVB irradiation. (A) Western blot analysis of the expression level of Bag-1/S in HaCaT, Le/GFP, Le/CIRP, and Le/Bag-1/S cells. (B) Western blot analysis of Tyr705-phosphorylated Stat3 (p-Stat3) and Bag-1/S in total cell lysates prepared from the indicated cell lines that are shame treated or treated with UVB and/or S3I-201 for 24 h. (C) Cell viability was measured at 24 h after the treatment using MTT assay. Results are the mean ± SD (error bar) from three independent experiments. *$P < 0.05$ versus untreated Le/GFP cells. #$P < 0.01$ versus UVB alone treated Le/GFP cells. $^{\hat{=}}P < 0.05$ versus UVB alone treated Le/Bag-1/S cells. $^{\Lambda}P < 0.01$ versus corresponding UVB/S3I-201 double-treated Le/GFP cells.

downstream regulator in preventing UVB-induced apoptosis.

To further verify the anti-apoptotic effect of CIRP, we analyzed the PARP cleavage and caspase 3 activation in UVB (7 mJ/cm^2) irradiated Le/CIRP cells, which overexpress CIRP (Figure 10A). Our data showed that while overexpression of CIRP did not have a significant effect on the apoptotic markers

(Figure 10A, Lanes 3 vs. 1), it could completely inhibit UVB-induced PARP cleavage and partly inhibit caspase 3 activation (Figure 10A, Lanes 4 vs. 2). Meanwhile overexpression of Bag-1/S could not only completely inhibit UVB-induced PARP cleavage and also caspase 3 activation (Figure 10B, Lanes 4 vs. 2). These result confirms that CIRP/Bag-1/S cassette suppresses UVB-induced apoptosis of keratinocytes.

Table 3. Relative Expression Levels of p-Stat3, Stat3, and Bag-1/S

	Le/GFP				Le/CIRP				Le/Bag-1/S			
UVB	−	+	−	+	−	+	−	+	−	+	−	+
S3I-201	−	−	+	+	−	−	+	+	−	−	+	+
p-Stat3	1	1.91 ± 0.43	0.80 ± 0.18	0.48 ± 0.14	1	1.71 ± 0.14	0.45 ± 0.04	0.38 ± 0.07	1	0.70 ± 0.04	0.33 ± 0.04	0.21 ± 0.01
Stat3	1	1.05 ± 0.10	0.96 ± 0.14	0.66 ± 0.05	1	1.08 ± 0.02	0.84 ± 0.01	0.56 ± 0.01	1	0.97 ± 0.06	0.89 ± 0.03	0.62 ± 0.02
p-Stat3/Stat3	1	1.80 ± 0.24	0.83 ± 0.07	0.71 ± 0.15	1	1.58 ± 0.16	0.53 ± 0.05	0.68 ± 0.11	1	0.72 ± 0.03	0.38 ± 0.03	0.35 ± 0.03
Bag-1/S	1	1.88 ± 0.32	0.72 ± 0.12	0.26 ± 0.12	1	1.39 ± 0.1	0.86 ± 0.05	0.57 ± 0.15	1	1.04 ± 0.01	0.95 ± 0.04	0.98 ± 0.05
Lane	1	2	3	4	5	6	7	8	9	10	11	12

DISCUSSION

Previous studies indicated that CIRP was associated with several types of human cancer and played important roles in tissue cell proliferation and survival upon stress [5–8,22,23]. CIRP expression could be induced by UV irradiation [1,24], but its biological impact on UVB-exposed keratinocytes is not well known. In this study, we demonstrated for the first time that CIRP expression is elevated in all tested skin cancer cell lines including melanoma and non-melanoma cells (Figure 1); as well as in keratinocytes exposed to a relatively low dose of UVB (3–5 mJ/cm^2) acutely or chronically (Figures 1 and 2). In opposite, the higher dose of UVB (50 mJ/cm^2) reduced the expression of CIRP, which could be due to the inhibition of translation of the protein as we previously reported [17,25,26]. The potential role of CIRP in UVB-induced skin carcinogenesis was further indicated by its function in regulation of Tyr-705 phosphorylation of Stat3 and the expression of its downstream genes—cyclin D1 and VEGF (Figure 2), two factors that are well known for their roles in promoting oncogenic cell growth and survival [27–29]. Furthermore, we demonstrated that the CIRP-mediated Tyr705-phosphorylation of Stat3 is correlated to the growth and survival rate of keratinocytes post-UVB (Figures 4–6), which is consistent with the observation that the level of cyclin D1 and VEGF as well as c-Myc increased in UVB resistant HaCaTt cells (Figure 2). However, CIRP appeared to have no effect on the expression of c-Myc (Figure 4A), which is a downstream gene of Stat3 [30]. This could be due to CIRP specifically regulating the Tyr705-phosphorylatedStat3-activated pathway but not the total expression of Stat3 (Figure 5A).

After elucidating that the CIRP-p-Stat3 cascade is likely to regulate cell proliferation by controlling cyclin D1 and VEGF expressions post-UVB, we also determined the role of CIRP in regulation of apoptosis post-UVB. Our data indicated that CIRP deficiency did not affect expression of Bcl-2 (Figure 4A), whose activity was suggested to be regulated by CIPR [31]. Our further study demonstrated that CIRP regulates Bag-1/(L, M, and S) expression (Figures 5 and 6); and the Bag-1/S expression appears to be dependent on the CIRP-mediated Tyr705-phosphorylation of Stat3 post-UVB irradiation (Figures 5, 7, and 8). It is worth to mention that some previous reports indicated that while p-Stat3 was rapid de-phosphorylated after UBV irradiation [11], it was observed in a higher level at longer period, from 1 to 6 d, post-UVB irradiation [13]. In our study, we observed a decrease of p-Stat3 at 6 h, and then an increase at 12–24 h after UVB irradiation. The early increase of CIRP associates a decrease of p-Stat3 could be due to that CIRP does not directly regulate the phosphorylation of Stat3, but is needed in regulation expression and/or activation of a kinase signaling pathway that regulates the recovery of Stat3
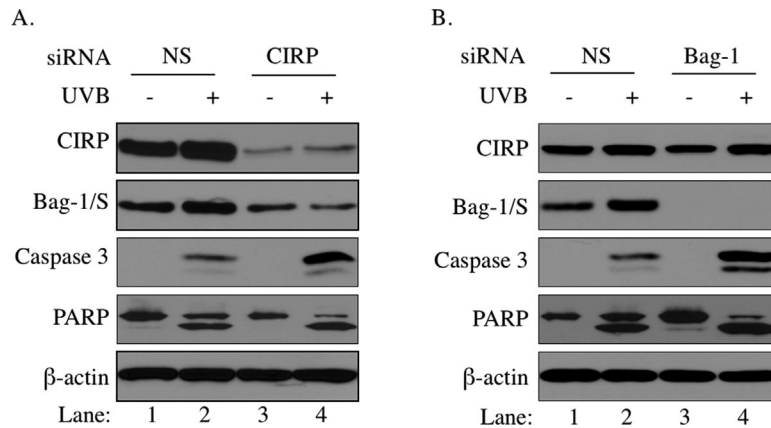
Figure 9. CIRP or Bag-1 knockdown sensitizes HaCaT cells to UVB-induced apoptosis. HaCaT cells transfected with NS siRNA or CIRP siRNA for 72 h (A), or transfected with NS siRNA or CIRP siRNA for 48 h (B) before receiving sham or UVB (7 mJ/cm²) irradiation. Total cell lysates were prepared at 24 h post-UVB irradiation. The levels of cleaved caspase 3 and PARP in the lysates were determined by western blot analysis.

phosphorylation post-UVB. Considering the RNA binding and facilitating target mRNAs translation characters of CIRP under stresses conditions, we believe this is a reasonable explanation for the role of CIRP in regulation of p-Stat3 after UVB irradiation.

While UVB increased the expression of Bag-1/S (Figure 8B, Lanes 2 vs. 1; 6 vs. 5; Table 3), it reduced the expression of Bag-1/S in the cells treated with S3I-201 (Figure 8B, Lanes 4 vs. 3; 8 vs. 7; Table 3), suggesting there are other mechanism(s) that also downregulate Bag-1/S expression post-UVB. Given that Stat3 mainly functions as a transcription activator [32], it is possible that the expression of Bag-1/S is regulated by the phosphorylation of Stat3 through transcription regulation and by phosphorylation of eIF2α through translation regulation as we previously

reported [17,25,26]. Our results further indicated that the CIRP-p-Stat3 cascade-upregulated expression of Bag-1/S protects the cells from UVB-induced PARP cleavage and caspase-3 activation (Figures 9 and 10), which agrees with previous reports indicating Bag-1/S is associated with stress resistance and anti-apopto-sis [20,33,34]. Based on our results, a novel mechanism for CIRP-p-Stat3 cascade-regulated cell growth and survival after UVB irradiation is proposed (Figure 11). Low dose UVB irradiation increases CIRP, which leads to the Tyr705-phosphorylation and activation of Stat3. In the event of a contingently enhanced Stat3 signaling pathway, the expressions of cyclin D1 and Bag-1/S increase, which promote keratinocyte growth and survival, which lead to clonal expansion or might eventually cause skin carcinogenesis.
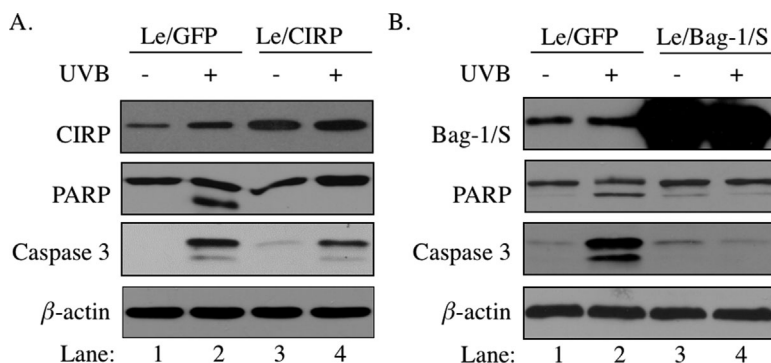

Figure 10. CIRP or Bag-1/S overexpression HaCaT is resistant to UVB-induced apoptosis. Western blot analysis of cleaved caspase 3 and PARP in total cell lysates prepared from Le/GFP and Le/CIRP cells that are shame treated or UVB (7 mJ/cm²) treated (A); or from same treated Le/GFP and Le/Bag-1/S cells (B).
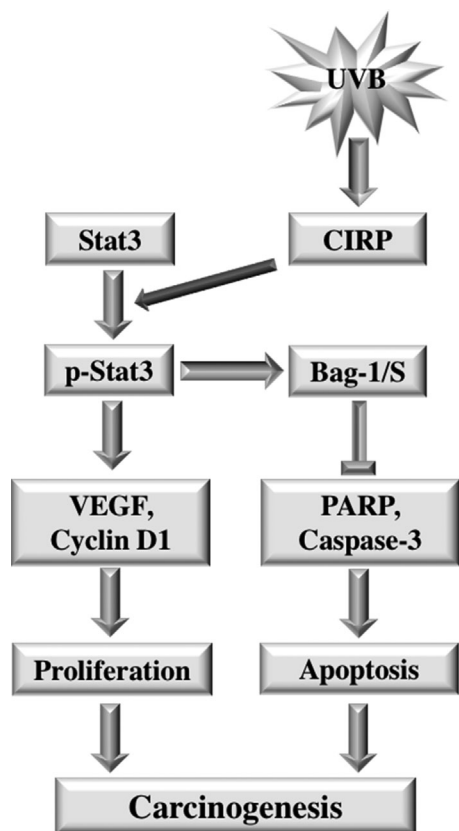
Figure 11. Proposed model for low-dose UVB-induced CIRP-mediated skin carcinogenesis.

ABBREVIATIONS

Bag-1	BCL2-associated athanogene
BAG-1/L	the largest isoform of Bag-1
BAG-1/M	the intermediate isoform of Bag-1
BAG-1/S	the most abundant isform of Bag-1
Caspase-3	cysteine-aspartic acid protease 3
CIRP	cold inducible RNA binding protein
CSPs	cold shock proteins
Cyclin D1	cell cycle protein D1
C-Myc	cellular-myelocytomatosis viral onco-gene
IOD	integrated optical density
LDH	lactate dehydrogenase
MTT	4,5-dimethyl-2-thiazolyl)-2,5-diphenyl-2-H-tetrazolium bromide
PARP	poly-(ADP-ribose) polymerase
p-Stat3	phosphorylated Stat3 at Tyr705
Stat3	signal transducer and activator of transcription 3
VEGF	vascular endothelial growthfactor

AUTHOR'S CONTRIBUTIONS

Mr. Yi Liao and Jianguo Feng contributed equally in this study performing the experiments in the

laboratories of Drs. Liling Tang and Shiyong Wu; and preparing the first draft of the manuscript. Ms. Yi Zhang assisted to culture cells and analyze the data. Drs. Tang and Wu instructed, supervised, and acquired funding to support the research; as well as prepared and finalized the manuscript.

REFERENCES

1. Sheikh MS, Carrier F, Papathanasiou MA, et al. Identification of several human homologs of hamster DNA damage-inducible transcripts. Cloning and characterization of a novel UV-inducible cDNA that codes for a putative RNA-binding protein. J Biol Chem 1997;272:26720–26726.
2. Xue JH, Nonoguchi K, Fukumoto M, et al. Effects of ischemia and H2O2 on the cold stress protein CIRP expression in rat neuronal cells. Free Radic Biol Med 1999;27:1238–1244.
3. Morf J, Rey G, Schneider K, et al. Cold-inducible RNA-binding protein modulates circadian gene expression posttranscriptionally. Science 2012;338:379–383.
4. De Leeuw F, Zhang T, Wauquier C, Huez G, Kruys V, Gueydan C. The cold-inducible RNA-binding protein migrates from the nucleus to cytoplasmic stress granules by a methylation-dependent mechanism and acts as a translational repressor. Exp Cell Res 2007;313:4130–4144.
5. Sakurai T, Itoh K, Higashitsuji H, et al. Cirp protects against tumor necrosis factor-alpha-induced apoptosis via activation of extracellular signal-regulated kinase. Biochim Biophys Acta 2006;1763:290–295.
6. Artero-Castro A, Callejas FB, Castellvi J, et al. Cold-inducible RNA-binding protein bypasses replicative senescence in primary cells through extracellular signal-regulated kinase 1 and 2 activation. Mol Cell Biol 2009;29:1855–1868.
7. Sakurai T, Kashida H, Watanabe T, et al. Stress response protein cirp links inflammation and tumorigenesis in colitis-associated cancer. Cancer Res 2014;74:6119–6128.
8. Sakurai T, Yada N, Watanabe T, et al. Cold-inducible RNA-binding protein promotes the development of liver cancer. Cancer Sci 2015;106:352–358.
9. Bowman T, Garcia R, Turkson J, Jove R. STATs in oncogenesis. Oncogene 2000;19:2474–2488.
10. Levy DE, Darnell JE, Jr. Stats: Transcriptional control and biological impact. Nat Rev Mol Cell Biol 2002;3:651–662.
11. Sano S, Chan KS, Kira M, et al. Signal transducer and activator of transcription 3 is a key regulator of keratinocyte survival and proliferation following UV irradiation. Cancer Res 2005;65:5720–5729.
12. Kim DJ, Angel JM, Sano S, DiGiovanni J. Constitutive activation and targeted disruption of signal transducer and activator of transcription 3 (Stat3) in mouse epidermis reveal its critical role in UVB-induced skin carcinogenesis. Oncogene 2009;28:950–960.
13. Lee H, Morales LD, Slaga TJ, Kim DJ. Activation of T-cell protein-tyrosine phosphatase suppresses keratinocyte survival and proliferation following UVB irradiation. J Biol Chem 2015;290:13–24.
14. Oishi N, Yamashita T, Kaneko S. Molecular biology of liver cancer stem cells. Liver Cancer 2014;3:71–84.

15. Liu K, Jiang M, Lu Y, et al. Sox2 cooperates with inflammation-mediated Stat3 activation in the malignant transformation of foregut basal progenitor cells. Cell Stem Cell 2013;12:304–315.
16. Reya T, Morrison SJ, Clarke MF, Weissman IL. Stem cells, cancer, and cancer stem cells. Nature 2001;414:105–111.
17. Tong L, Wu S. The role of constitutive nitric-oxide synthase in ultraviolet B light-induced nuclear factor kappaB activity. J Biol Chem 2014;289:26658–26668.
18. Brochu C, Cabrita MA, Melanson BD, et al. NF-kappaB-dependent role for cold-inducible RNA binding protein in regulating interleukin 1beta. PLoS ONE 2013;8:e57426.
19. Tang SC. BAG-1, an anti-apoptotic tumour marker. IUBMB Life 2002;53:99–105.
20. Dobbyn HC, Hill K, Hamilton TL, et al. Regulation of BAG-1 IRES-mediated translation following chemotoxic stress. Oncogene 2008;27:1167–1174.
21. Siddiquee K, Zhang S, Guida WC, et al. Selective chemical probe inhibitor of Stat3, identified through structure-based virtual screening, induces antitumor activity. Proc Natl Acad Sci USA 2007;104:7391–7396.
22. Wu Y, Guo X, Brandt Y, Hathaway HJ, Hartley RS. Three-dimensional collagen represses cyclin E1 via beta1 integrin in invasive breast cancer cells. Breast Cancer Res Treat 2011;127:397–406.
23. Guo X, Wu Y, Hartley RS. Cold-inducible RNA-binding protein contributes to human antigen R and cyclin E1 deregulation in breast cancer. Mol Carcinog 2010;49:130–140.
24. Fornace AJ, Alamo I, Jr., Hollander MC, Jr. DNA damage-inducible transcripts in mammalian cells. Proc Natl Acad Sci USA 1988;85:8800–8804.
25. Wu S, Hu Y, Wang JL, Chatterjee M, Shi Y, Kaufman RJ. Ultraviolet light inhibits translation through activation of the unfolded protein response kinase PERK in the lumen of the endoplasmic reticulum. J Biol Chem 2002;277:18077–18083.
26. Lu W, Laszlo CF, Miao Z, Chen H, Wu S. The role of nitric-oxide synthase in the regulation of UVB light-induced phosphorylation of the alpha subunit of eukaryotic initiation factor 2. J Biol Chem 2009;284:24281–24288.
27. Kim AL, Athar M, Bickers DR, Gautier J. Stage-specific alterations of cyclin expression during UVB-induced murine skin tumor development. Photochem Photobiol 2002;75:58–67.
28. Deng J, Cui J, Jiang N, et al. STAT3 regulation the expression of VEGF-D in HGC-27 gastric cancer cell. Am J Transl Res 2014;6:756–767.
29. el Filali M, van der Velden PA, Luyten GP, Jager MJ. Anti-angiogenic therapy in uveal melanoma. Dev Ophthalmol 2012;49:117–136.
30. Lui GY, Kovacevic Z, V Menezes S, et al. Novel thiosemi-carbazones regulate the signal transducer and activator of transcription 3 (STAT3) pathway: Inhibition of constitutive and interleukin 6-induced activation by iron depletion. Mol Pharmacol 2015;87:543–560.
31. Lee HN, Ahn SM, Jang HH. Cold-inducible RNA-binding protein, CIRP, inhibits DNA damage-induced apoptosis by regulating p53. Biochem Biophys Res Commun 2015;464:916–921.
32. Akira S, Nishio Y, Inoue M, et al. Molecular cloning of APRF, a novel IFN-stimulated gene factor 3 p91-related transcription factor involved in the gp130-mediated signaling pathway. Cell 1994;77:63–71.
33. Aveic S, Viola G, Accordi B, et al. Targeting BAG-1: A novel strategy to increase drug efficacy in acute myeloid leukemia. Exp Hematol 2015;43:180–190 e186.
34. Townsend PA, Cutress RI, Sharp A, Brimmell M, Packham G. BAG-1 prevents stress-induced long-term growth inhibition in breast cancer cells via a chaperone-dependent pathway. Cancer Res 2003;63:4150–4157.

SUPPORTING INFORMATION

Additional supporting information may be found in the online version of this article at the publisher's web-site.